



Cite this: *Environ. Sci.: Nano*, 2026, 13, 1601

Emerging investigator series: environmental safety assessment of 11 novel metal oxide/hydroxide nanocomposite adsorbents for advanced magnetic removal and recovery of phosphorus from wastewater

Asya Drenkova-Tuhtan, *^a Irina Blinova,^a Mariliis Sihtmäe, ^a Villem Aruoja, ^a Alla Khosrovyan ^a and Anne Kahru ^{ab}

This study evaluated the ecotoxicity of 11 metal oxide/hydroxide nanocomposite adsorbents for advanced magnetic removal/recovery of phosphorus from wastewater using four test organisms representing different aquatic trophic levels: bacteria *Vibrio fischeri*, crustaceans *Daphnia magna*, algae *Raphidocelis subcapitata* and midge *Chironomus riparius* larvae. The nanocomposites ($d_{50} < 10 \mu\text{m}$) were synthesized as co-precipitates of 2-, 3- and/or 4-valent metal precursors (Zn^{2+} , Ca^{2+} , Mg^{2+} , Fe^{3+} , Zr^{4+}) at varying molar ratios. The shedding of precursor metals in toxic concentrations was observed only for the Zn-containing adsorbents. The acute toxicity of the Zn-containing composites ranged from “harmful” to bacteria ($10 < 30 \text{ min EC}_{50} \leq 100 \text{ mg L}^{-1}$), “toxic” to crustaceans ($1 < 48 \text{ h EC}_{50} \leq 10 \text{ mg L}^{-1}$) and “very toxic” to midge larvae and algae ($24 \text{ h LC}_{50} \leq 1 \text{ mg L}^{-1}$). As a rule, their toxicity correlated with the concentration of shed Zn-ions. All nanocomposites, regardless of their composition, proved very toxic to algae, *i.e.* remarkably inhibited algal growth ($72 \text{ h EC}_{50} \leq 1 \text{ mg L}^{-1}$). The latter effect could be explained by (i) shed Zn-ions in case of Zn-containing materials as algae are very sensitive to heavy metals, (ii) composites-induced phosphorus removal from the algal growth medium and (iii) entrapment of algal cells into particle agglomerates. Importantly, the most-promising benchmark material ZnFeZr-6:1:1 (*V. fischeri* $\text{EC}_{50} = 118 \text{ mg L}^{-1}$; *D. magna* $\text{EC}_{50} = 7.7 \text{ mg L}^{-1}$; *C. riparius* $\text{LC}_{50} = 0.59 \text{ mg L}^{-1}$) proved safe for bacteria and crustaceans once deposited on magnetic particles ZnFeZr-6:1:1@MPs yielding $\text{EC}_{50} > 100 \text{ mg L}^{-1}$. Summing up, although Zn enhances the adsorbent selectivity and reusability, all Zn-containing P-adsorbents are questionable in terms of ecosafety and thus not recommended for engineering applications in open systems.

Received 24th September 2025,
Accepted 18th February 2026

DOI: 10.1039/d5en00887e

rsc.li/es-nano

Environmental significance

Advanced nanostructured materials for efficient removal/recovery of phosphorus (P) from wastewater are in growing demand, driven by the new EU Urban Wastewater Treatment Directive (UWWTD-2024/3019), which introduces stricter P-discharge limits and mandates P-recovery, as an environmental pollutant causing eutrophication, but also a key nutrient for agriculture. Engineered nanocomposite metal oxide/hydroxide-based materials are excellent phosphate adsorbents, selectively removing P from wastewater to ultra-low concentrations and enabling P-recovery through reversible sorption. Nevertheless, their potential ecotoxicological hazard to aquatic organisms if discharged in the environment is considerably overlooked. To assure their “safe-by-design” nature, this study assesses the environmental safety of 11 highly efficient metal oxide/hydroxide nanocomposite P-adsorbents using toxicity assays with 4 model organisms representing different trophic levels of the aquatic food-web.

1. Introduction

Advanced materials for efficient water and wastewater treatment are in growing demand, driven by the rapidly changing world and the need for sustainable, holistic and integrated water management solutions towards circular economy (resource

^a Laboratory of Environmental Toxicology, National Institute of Chemical Physics and Biophysics, Akadeemia tee 23, 12618 Tallinn, Estonia.

E-mail: asya.drenkova@kbfi.ee

^b Estonian Academy of Sciences, Kohtu 6, 10130 Tallinn, Estonia



recovery, water reuse) and enhanced aquatic ecosystems protection.

Wastewater treatment plants (WWTPs) are no longer considered end-of-pipe waste facilities, but rather water and resources recovery factories (WRRFs), offering significant untapped potential for “urban mining” and secondary resource recovery (nutrients, energy, water, *etc.*). Nevertheless, the priority task of WWTPs is, first and foremost, to treat reliably and dispose safely the wastewater effluent, complying with the regulatory discharge limit values.

The recently adopted recast of the EU Urban Wastewater Treatment Directive (UWWTD 2024/3019 replacing 1991/271) was approved by the European Council in November 2024.¹ It sets new ambitious goals for WWTPs, including energy neutrality, advanced quaternary treatment for removal of organic micropollutants and emerging contaminants (pharmaceuticals, cosmetics, microplastics, *etc.*), more stringent discharge limits, respectively stricter removal requirements for the nutrients phosphorus (P) and nitrogen (N), and mandatory phosphorus recovery from sewage sludge and wastewater. The minimum combined P-reuse and recycling targets will be defined by January 2028.

The new discharge limit values for phosphorus go down to 0.5 mg L⁻¹ P-total for WWTPs >10 000 p.e. (population equivalents), which is economically difficult to achieve with conventional treatment techniques like chemical precipitation with metal salts or enhanced biological phosphorus removal (EBPR). Sorption, as an alternative, is one of the most effective methods for removal of dissolved compounds, especially in the low concentration range of µg L⁻¹–mg L⁻¹.² As demonstrated in our recent research, with the help of engineered reusable nanocomposite adsorbents combining various 2-, 3- and 4-valent metals (Ca²⁺, Mg²⁺, Zn²⁺, Fe³⁺, Zr⁴⁺) co-precipitated as oxides/hydroxides, it is possible to tackle simultaneously both goals in the new UWWTD 2024/3019, namely total P removal to ultra-low concentrations <0.05 mg L⁻¹ P-total and complete *ortho*-phosphate elimination <LOD = 0.005 mg L⁻¹ PO₄-P,³ including complete removal of non-reactive P-species (<LOD = 0.015 mg L⁻¹ P-total) such as the recalcitrant phosphonates NTMP and DTPMP,⁴ and P recovery as a valuable fertilizer product like struvite (MgNH₄PO₄·6H₂O).⁵

Combining various metals in one nanocomposite material makes the adsorbent more efficient and selective towards phosphate with adsorption capacity >50 mg P per g-adsorbent,⁶ reaching up to 94 mg P per g-adsorbent for the most-promising material ZnFeZr-6:1:1 in real wastewater, and improves its long-term reusability (60+ cycles) after alkaline regeneration without compromising adsorption efficiency,⁵ which is essential for practical engineering applications. Furthermore, we were able to successfully immobilize the best-performing adsorbent on magnetic carrier particles (denoted as ZnFeZr-6:1:1@MPs) to facilitate its easier harvesting and regeneration, and to produce several kilograms of it, demonstrating the scalability of the synthesis process.⁷ In contrast, other studies on composite magnetic P-adsorbents report adsorption capacity typically <50 mg P per g-adsorbent in synthetic solutions (not real

wastewater) at small lab-scale and rarely demonstrate successful regeneration of the materials beyond 4–5 cycles, often resulting in a significant loss of adsorption capacity (>40%) after several reuse cycles.⁸

Nevertheless, the direct application of these nanocomposite adsorbents as a last treatment stage, before discharging the WWTP effluent, raises concerns about their environmental safety to aquatic organisms if accidentally discharged in the environment. The uncertainty regarding possible ecotoxicological hazards arising from the use of these custom materials has produced new research gaps addressed in this study.

The current study is a follow-up to our previous work,⁹ where we synthesized 11 nanocomposite adsorbents and investigated their stability under different physiochemical conditions, focusing on the leaching of potentially hazardous metal ions. Using an ecotoxicological screening assay that explores the naturally luminescent bacteria *Vibrio fischeri* as a model organism,¹⁰ we revealed that only the Zn-containing adsorbents showed bacterial bioluminescence inhibition (*i.e.* toxic) effects. Furthermore, we varied the amount of Zn²⁺ incorporated in the structure of the previously tested best-performing adsorbent combination Zn²⁺Fe³⁺Zr⁴⁺ by gradually reducing the Zn-fraction to avoid the leaching of zinc ions, which are toxic to several key aquatic organisms groups,¹¹ without compromising the P-adsorption capacity of the material. Zinc is a heavy metal with high aquatic toxicity potency which is provenly toxic to bacteria *Vibrio fischeri* and crustacean *Daphnia magna* at concentrations <10 mg L⁻¹ (comparable with the Zn²⁺ leached from the nanocomposite prototypes) and highly toxic to algae already at µg L⁻¹ level (see Table S5 in SI). The presence of zinc, however, is necessary to enhance the adsorption selectivity towards phosphate.⁷ Thus, the 11 adsorbents synthesized in our previous work⁹ and listed in Table 1 include five variations of the Zn²⁺Fe³⁺Zr⁴⁺ material, five additional combinations with other 2-valent metals (Ca²⁺ or Mg²⁺) to either replace or complement zinc (Zn²⁺) in the composite structure, and one magnetic adsorbent ZnFeZr-6:1:1@magnetic particles (MPs). The magnetized version of the most promising P-adsorbent, denoted as ZnFeZr-6:1:1@MPs (benchmark), is the first material prototype whose synthesis was successfully upscaled to kg-range production in a pilot test and is also tested for toxicity.

The pre-screening for ecotoxicity with bacteria *Vibrio fischeri* showed that the luminescent bacteria were sensitive only to the Zn-containing compounds, which motivated us to perform 3 additional bioassays with more sensitive test organisms. In the current work, we advance further the environmental safety assessment of the above described 11 novel adsorbents by investigating their potential harmful effects on other model test organisms representing different trophic levels of the aquatic food-web, such as crustacean *Daphnia magna*, green freshwater microalgae *Raphidocelis subcapitata* (formerly *Pseudokirchneriella subcapitata* and *Selenastrum capricornutum*) and larvae of sediment-dwelling freshwater non-biting midge *Chironomus riparius*. Notably,





Table 1 Physicochemical properties of the as-synthesized metal oxide/hydroxide nanocomposites tested in this study

| Composite name | Measured molar ratios of metal precursors (ICP-OES analysis) | | | | | | Zn-fraction by molar mass (wt%) | Primary particle size d_{50} (μm) | ζ -Potential in DI water (mV) | pH in DI water (-) |
|--|--|------------------|------------------|------------------|------------------|------------------|---------------------------------|--|-------------------------------------|--------------------|
| | Ca ²⁺ | Mg ²⁺ | Zn ²⁺ | Fe ³⁺ | Zr ⁴⁺ | Zr ⁴⁺ | | | | |
| ZnFeZr-18:5:1 | n.a. | n.a. | 20.26 ± 1.22 | 5.83 ± 0.15 | 1.00 ± 0.00 | 36.6 ± 4.7 | 3.7 | +27.2 ± 0.8 | 6.7 | |
| ZnFeZr-10:1:1 | n.a. | n.a. | 10.74 ± 0.55 | 1.15 ± 0.09 | 1.00 ± 0.00 | 37.0 ± 3.8 | 5.5 | +13.7 ± 1.4 | 6.5 | |
| ZnFeZr-6:1:1 (benchmark – active component) | n.a. | n.a. | 6.41 ± 0.01 | 1.16 ± 0.01 | 1.00 ± 0.00 | 26.2 ± 1.3 | 4.5 | +9.2 ± 0.1 | 6.7 | |
| ZnFeZr-4:1:1 | n.a. | n.a. | 4.01 ± 0.13 | 1.14 ± 0.04 | 1.00 ± 0.00 | 24.1 ± 3.4 | 9.9 | +14.6 ± 2.8 | 6.9 | |
| ZnFeZr-3:6:0.2:1 | n.a. | n.a. | 3.44 ± 0.08 | 0.23 ± 0.04 | 1.00 ± 0.00 | 25.4 ± 2.4 | 8.1 | +8.3 ± 0.1 | 6.6 | |
| CaFe-2:1 | 0.05 ± 0.01 | n.a. | n.a. | 1.00 ± 0.00 | n.a. | n.a. | 4.0 | +9.2 ± 0.9 | 8.0 | |
| CaFeZr-6:1:1 | 0.12 ± 0.01 | n.a. | n.a. | 1.14 ± 0.01 | 1.00 ± 0.00 | n.a. | 6.0 | -9.0 ± 0.1 | 7.9 | |
| CaZnFeZr-3:3:1:1 | 0.00 ± 0.01 | n.a. | 2.73 ± 0.08 | 1.14 ± 0.07 | 1.00 ± 0.00 | 18.3 ± 2.4 | 5.9 | +9.5 ± 0.1 | 6.5 | |
| MgFeZr-6:1:1 | n.a. | 0.22 ± 0.01 | n.a. | 1.15 ± 0.05 | 1.00 ± 0.00 | n.a. | 9.5 | -12.2 ± 0.4 | 8.1 | |
| MgZnFe-1:1:1 | n.a. | 0.31 ± 0.02 | 0.95 ± 0.07 | 1.00 ± 0.00 | n.a. | 16.7 ± 1.5 | 3.2 | +27.7 ± 0.6 | 7.2 | |
| ZnFeZr-6:1:1@MPS (benchmark – magnetized) | n.a. | n.a. | 4.88 ± 0.35 | 53.09 ± 1.51 | 1.00 ± 0.00 | 5.2 ± 0.3 | >20.0 | — | 7.0 | |

Remark: primary particle size distribution analysis was performed with laser diffraction and results are reported as median diameter d_{50} , μm (see also plots in Fig. S2). The surface charge (ζ -potential) and pH were measured in 100 mg L⁻¹ suspensions in DI water with Malvern Zetasizer Nano-ZS (Malvern instruments, UK) utilizing electrophoretic light scattering (ELS). Values are average of three measurements ($n = 3$) and are adopted from ref. 9 (open access publication). n.a. – “not applicable”.

both *Daphnia magna* and *Raphidocelis subcapitata* are model organisms recommended for chemical safety assessment under the REACH regulation.¹² The acute assay with *Chironomus riparius* larvae (standard model organism used for testing dissolved and insoluble chemicals) was set-up to compare the response of a sediment-dwelling organism with those of the aquatic species crustacean *D. magna* and microalgae *R. subcapitata*, and this was performed only for 3 representative Zn-containing materials that already showed toxicity to *D. magna* and *R. subcapitata* to avoid excessive testing.

Furthermore, in addition to the *Vibrio fischeri* bioluminescence inhibition assay¹⁰ and the algal growth inhibition assay,¹³ a ‘Spot Test’ (viability assay) was carried out to provide complementary toxicity endpoints to algal growth inhibition test as well as to *V. fischeri* bioluminescence inhibition test by assessing the ability of test organisms to grow (form colonies) after exposure to the nanocomposites. For example, the algal growth inhibition test just detects the reduction of algal biomass as a function of increasing toxicant concentration without differentiating between the different toxicity mechanisms. As indirect toxic effects may occur from e.g. nutrients removal (by forming insoluble complexes with phosphorus) or from physical entrapment of algae into agglomerates, a viability assay will provide a more realistic estimate of all living algal biomass, even if it is physically entrapped or nutrients depleted.

Performing several bioassays with different test species provides a more comprehensive and realistic environmental safety evaluation of these novel materials in the context of the “Safe-and-Sustainable-by-Design” (SSbD) principle.¹⁴ Such evaluation is meant to support a decision-making process when choosing between different alternative materials with similar functionality, namely different adsorbents offering the same function of efficient, selective, reversible and robust phosphate adsorption with long-term reusability. The formation of the alternative adsorbents is based on our very first screening study⁶ following the hypothesis that the adsorbents can be made “Safe-and-Sustainable-by-Design” by reducing the content/leaching of Zn while maintaining the adsorptive properties. The main goal of this study, which addresses one part of the SSbD framework, is to advance the commercialization of the proposed P-removal and recovery technology by proactively verifying its environmentally friendly application, and the compliance of the adsorbents with the SSbD principle.

2. Materials and methods

2.1. Synthesis and characterization of 11 metal oxide/hydroxide nanocomposites adsorbents for advanced wastewater treatment

The synthesis and full characterization of all studied nanocomposite materials was already reported in our previously published work.⁹ In brief, the nanocomposites were synthesized through alkaline co-precipitation of pre-dissolved metal salts of

Table 2 Solubility of the nanocomposites – metal concentrations measured with TXRF in 0.1 μm -filtered supernatants of 1 g L^{-1} particle suspensions in deionized (DI) water

| Composites (1 g L^{-1} suspensions) | Shedding of solubilized metal ions (mg L^{-1}) | | | | |
|--|---|-------------------|------------------|-------------------|--------------------|
| | Zn ²⁺ | Fe ³⁺ | Zr ⁴⁺ | Ca ²⁺ | Mg ²⁺ |
| ZnFeZr-18:5:1 | 6.870 \pm 0.025 | 0.032 \pm 0.005 | <LOD | n.a. | n.a. |
| ZnFeZr-10:1:1 | 4.564 \pm 0.022 | 0.015 \pm 0.005 | <LOD | n.a. | n.a. |
| ZnFeZr-6:1:1 | 20.494 \pm 0.060 | 0.028 \pm 0.010 | <LOD | n.a. | n.a. |
| ZnFeZr-4:1:1 | 10.861 \pm 0.028 | 0.035 \pm 0.004 | <LOD | n.a. | n.a. |
| ZnFeZr-3.6:0.2:1 | 5.352 \pm 0.020 | 0.012 \pm 0.004 | <LOD | n.a. | n.a. |
| CaFe-2:1 | n.a. | 0.083 \pm 0.005 | n.a. | 9.893 \pm 0.081 | n.a. |
| CaFeZr-6:1:1 | n.a. | 0.030 \pm 0.004 | <LOD | 5.992 \pm 0.058 | n.a. |
| CaZnFeZr-3:3:1:1 | 25.736 \pm 0.058 | <LOD | <LOD | <LOD | n.a. |
| MgFeZr-6:1:1 | n.a. | 0.013 \pm 0.004 | <LOD | n.a. | <LOD |
| MgZnFe-1:1:1 | 0.075 \pm 0.004 | 0.041 \pm 0.005 | n.a. | n.a. | 15.330 \pm 5.845 |
| ZnFeZr-6:1:1@MPs | 1.095 \pm 0.021 | 0.105 \pm 0.015 | <LOD | n.a. | n.a. |

Remark: the Zr⁴⁺ values were below the limit of detection (<LOD) in ppb range for all samples. Values are average of minimum two measurements with maximum 5% deviation and are adopted from ref. 9 (open access publication). n.a. – “not applicable”.

two, three and four-valent metal precursors (Ca²⁺, Mg²⁺, Zn²⁺, Fe³⁺, Zr⁴⁺) at different molar ratios. The metal salts calcium chloride dihydrate (CaCl₂·2H₂O), magnesium chloride hexahydrate (MgCl₂·6H₂O), zinc chloride (ZnCl₂) and iron(III) chloride hexahydrate (FeCl₃·6H₂O) were purchased from VWR Chemicals (Germany). Zirconium(IV) oxychloride octahydrate (ZrOCl₂·8H₂O) was obtained from Sigma-Aldrich (Germany). Sodium hydroxide (NaOH) and hydrochloric acid (HCl, 37%) for the particles synthesis was purchased also from VWR Chemicals (Germany). All chemicals were reagent grade ($\geq 98\%$ purity) and used as received. The precursor solutions were prepared by dissolving the respective metal salt in 100 mL deionized water. The obtained solution was added drop-by-drop using a peristaltic pump (1.4 mL min⁻¹) to 400 mL of 0.15 M NaOH in a 1 L round flask under stirring (300 rpm) within 10 minutes, maintaining pH >10 the whole time to ensure that all metals are precipitated to oxides/hydroxides. The resulting turbid suspension was stirred for another 5 minutes at this highly alkaline pH and then it was neutralized to pH 7 with 37% HCl to stop the reaction. After this step, all samples were centrifuged (5000 rpm), washed twice with deionized water, dispersed in 200 mL deionized water and stored as aqueous suspensions.

All as-synthesized materials were characterized accordingly using laser diffraction, SEM, XRD and ICP-OES. The laser diffraction particle size distribution analysis showed median diameter (primary size) in the range $d_{50} = 1\text{--}10 \mu\text{m}$ for all as-synthesized nanocomposites, with secondary peaks $\sim 100\text{--}300 \text{ nm}$, indicating the presence of nanoparticles in some of the structures. The composites' stability was investigated in deionized water and in 2% NaCl addressing agglomeration, settling and solubilization. The composites' particle settling and solubility tests were performed at concentrations 1–1000 mg L^{-1} (referring to the whole composite mass). The settling ability was assessed qualitatively by taking static time-lapse photographs at settling times 0 min, 30 min, 4 h and 24 h which are relevant exposure times for the bioassays (see Fig. S4 in the SI). Solubility of the nanocomposites (1000 mg L^{-1} suspensions) was analyzed further only in deionized water

after 0.1 μm sample filtration (cellulose acetate filter Minisart®, Sartorius-Stedim-Biotech GmbH) to separate the particles from the soluble fraction. The respective metal concentrations in the filtrates were measured using total reflection X-ray fluorescence spectrometer (TXRF; Picofox-S2, Bruker-Nano GmbH, Germany) and relevant data is included in Table 2. The XRD data revealed presence of hazardous ZnO nanoparticles in the structures with the highest Zn-fraction, and the stability test results showed that all Zn-containing materials leached Zn²⁺ ions.⁹ Thus, further synthesis modifications were made to reduce the Zn-fraction in the materials structure to minimize the leaching of Zn²⁺ which can be harmful to aquatic organisms (see Introduction).

Finally, five variations of the previously pilot-scale tested⁵ and highly promising P-adsorbent ZnFeZr-nanocomposite were synthesized with nominal molar ratios Zn²⁺:Fe³⁺:Zr⁴⁺ = 18:5:1; 10:1:1; 6:1:1; 4:1:1 and 3.6:0.2:1. Furthermore, five additional hydroxide composites were synthesized by incorporating other 2-valent metals (Ca²⁺ or Mg²⁺) to replace or complement Zn²⁺ in the material structure, namely Ca²⁺:Fe³⁺ = 2:1; Ca²⁺:Fe³⁺:Zr⁴⁺ = 6:1:1; Ca²⁺:Zn²⁺:Fe³⁺:Zr⁴⁺ = 3:3:1:1; Mg²⁺:Fe³⁺:Zr⁴⁺ = 6:1:1 and Mg²⁺:Zn²⁺:Fe³⁺ = 1:1:1.

Moreover, the magnetic version of the most-promising P-adsorbent, denoted as ZnFeZr-6:1:1@MPs (benchmark – magnetized), was also included in the tests. On a lab-scale, the deposition of the ZnFeZr-adsorbent on magnetic particles was performed through co-precipitation at room temperature and ambient pressure. For this purpose, 27 g of magnetite (Fe₃O₄) magnetic particles were dispersed in 1.4 L deionized water under stirring. Then 17.6 g (129 mmol) of ZnCl₂, 5.9 g (21.8 mmol) of FeCl₃·6H₂O and 6.9 g (21.4 mmol) of ZrOCl₂·8H₂O were dissolved in 550 mL deionized water and added to the magnetite particle dispersion. The resultant dispersion and 2.0 L of 0.15 M NaOH solution were pumped together through a Y-piece with a peristaltic pump, leading to precipitation of the metal salts on the particle surface. The functionalized particles were then washed with deionized water several times until the pH-value was neutral.



Overall, 11 different metal oxide/hydroxide nanocomposite adsorbents listed in Table 1 were synthesized in our previous work⁹ and exposed to a comprehensive aquatic toxicity testing in this study.

2.2. Preparation of the metal oxides/hydroxides particle suspensions and analysis of metal solubility

For the preparation of the stock suspensions (100 mg L⁻¹ in the general case and 1 g L⁻¹ for the bacterial 'Spot Test'; see below), the nanocomposites were suspended in the corresponding test medium, sonicated for 2 min at 40 W, 20 kHz (450 Ultrasonifier probe sonicator, Branson-Ultrasonics-Corporation, USA) and vortexed before preparation of the test series dilutions on the same day.

The composites' surface charge (ζ -potential) was measured in 100 mg L⁻¹ suspensions in deionized (DI) water (18.2 M Ω , pH 5.6 \pm 0.1, Milli-Q/Millipore, Billerica, USA) with Malvern Zetasizer Nano-ZS (Malvern Instruments, UK).

The metal solubility of the nanocomposites was analyzed for all precursor metals after 0.1 μ m filtration of pre-made 1 g L⁻¹ stock suspensions in DI water. First, 50 μ L of each filtrate was mixed with gallium (Ga) internal standard at 1:1 ratio and then, 5 μ L of the mixture was pipetted onto a quartz disk. The respective metal concentrations in the filtrates were measured using total reflection X-ray fluorescence (TRXF) spectrometer Picofox-S2 and quantified with Spectra-software 7.2.5.0 (Bruker-Nano GmbH, Germany). Furthermore, attention was focused on the concentration of total Zn (heavy metal with high aquatic toxicity potency), measured directly from the test media of all Zn-containing nanocomposites at the end of the toxicity tests. Samples were collected from the upper layer of the exposure medium at all test concentrations, avoiding re-suspension of the settled nanocomposites, and analyzed with TXRF.

The soluble precursors metal salts (ZnCl₂, FeCl₃·6H₂O, ZrOCl₂·8H₂O, CaCl₂·2H₂O and MgCl₂·6H₂O) used for the synthesis of the nanocomposite adsorbents were also tested for toxicity. Their 1 g L⁻¹ stock solutions in DI water had close to neutral pH 6.3–6.8, except for the highly acidic FeCl₃·6H₂O (pH 1.9) and ZrOCl₂·8H₂O (pH 1.8). The test concentrations of the latter two salts in the different test media still had acidic pH 3–5.5, which was outside the recommended range for the toxicity assays (pH 6–8.5). However, adjusting the pH with NaOH formed insoluble precipitates which discredited the toxicity results for these two salts.

Since all tested nanocomposites in this work were initially developed for the targeted adsorption of phosphate from aqueous media, an additional experiment showed that they rapidly removed all phosphate from the algae test/growth medium of the OECD-201 bioassay from PO₄ = 1.12 mg L⁻¹ in original medium¹³ to PO₄ < LOD after 1 h contact with the adsorbents, which is especially critical for green algae, as phosphorus is an essential nutrient and they do not grow without it. Importantly, growth inhibition of algae is a toxicity endpoint for that bioassay. Thus, four selected representative nanocomposites with and without zinc (ZnFeZr-6:1:1,

CaFeZr-6:1:1, MgFeZr-6:1:1, ZnFeZr-6:1:1@MPs) were purposefully pre-loaded with phosphate-phosphorus (P) until saturation (see Fig. S1 in SI), *i.e.* until inability to adsorb anymore phosphate. The saturated P-preloaded particles of the four selected nanocomposites were then exposed to the OECD-201 bioassay and the EC₅₀ results were compared against their virgin counterparts (fresh as-synthesized nanocomposites, not being exposed to phosphate adsorption). This helped to elucidate indirectly possible toxicity mechanisms. Particularly, it could be inferred if potential algal growth inhibition effects arise only from the lack of nutrients (specifically phosphorus), especially if there is no toxic zinc present in the adsorbent structure, by comparing the EC₅₀ values of *e.g.* virgin CaFeZr-6:1:1 (hypothesis: very toxic to algae due to spontaneous phosphorus uptake from the growth medium, *i.e.* due to nutrients depletion) *vs.* P-preloaded CaFeZr-6:1:1 (hypothesis: not toxic to algae because adsorbent is P-saturated and does not uptake phosphorus from the medium, and has no toxic Zn in its structure). The results are discussed in section 3.2.3.

2.3. Toxicity bioassays with model organisms representing different trophic levels of the aquatic food-web

2.3.1. *Vibrio fischeri* bioluminescence inhibition test (ISO-21338:2010).

The *Vibrio fischeri* acute kinetic bioluminescence inhibition assay was performed according to the modified Flash-assay standard ISO protocol¹⁰ at 30 min exposure time in 2% NaCl medium. The nominal concentration of a compound reducing the bacterial bioluminescence by 50% is defined as the half maximal effective concentration (EC₅₀), calculated as described in section 2.4.

Details of the test methodology and all toxicity data for *Vibrio fischeri* assay were reported in our earlier work.⁹ For convenience and comparability, a summary of key results is provided here, and the full method is described in S1.

2.3.2. Acute immobilization test with crustacean *Daphnia magna* (OECD-202).

The *Daphnia magna* assay was performed following the OECD-202 standard guideline for chemicals testing.¹⁵ All experiments were conducted in artificial freshwater solution (pH 7.8 \pm 0.2) containing 294 mg L⁻¹ CaCl₂·2H₂O, 123.25 mg L⁻¹ MgSO₄·7H₂O, 64.75 mg L⁻¹ NaHCO₃ and 5.75 mg L⁻¹ KCl. *Daphnia magna* dormant eggs were purchased from MicroBioTests, Inc. (Gent, Belgium). Neonates (<24 h old) hatched from the dormant eggs were pre-fed with a concentrated suspension of the microalga *Raphidocelis subcapitata* for 2 h prior to testing and exposed for 48 h to the nanocomposite suspensions at nominal concentrations 3.12, 6.25, 12.50, 25.00, 50.00 and 100.00 mg L⁻¹ in static test conditions (21 °C, in the dark). Overall, 2 to 4 independent tests were conducted with 4 replicates for each tested concentration. The 48 h EC₅₀ values (median effective substance concentration causing 50% immobilization of the test organisms) were calculated as described in section 2.4.

After the test, *Daphnia magna* specimens were examined under a Nikon-SMZ1270 microscope and photographed using a digital camera DS-Fi3 and software NIS-BR.



2.3.3. Algal growth inhibition assay with green freshwater microalgae *Raphidocelis subcapitata* (OECD-201). This bioassay was conducted following the OECD-201 guideline¹³ and detailed description in.¹⁶ The *Raphidocelis subcapitata* inoculum stock culture was purchased as commercial Algal-Toxkit-F from MicroBioTests Inc. (Gent, Belgium). Briefly, the number of algal cells in the inoculum was determined by counting under a light microscope and the initial cell density in all experiments was 5000–10 000 cells per mL. Exponentially growing algal cultures were exposed to various concentrations of the nanocomposite suspensions (or metal salts) and incubated at 24 ± 1 °C for 72 h in standard 20 mL glass scintillation vials with 15 mL sample each. The vials were shaken on a transparent table, illuminated from below at 6700–8900 lux with 3200 lm, 40 W SYLVANIA LED panel. In every test, algae were exposed to at least 5 toxicant concentrations in 3 replicates ($n = 3$), together with minimum 8 control replicates per experiment, distributed evenly on the table. All tests were repeated at least twice, always including CuSO_4 dilution series as a positive control.

The algal biomass was quantified by measuring chlorophyll *a* fluorescence every 24 h. First, 50 μL of well-homogenized samples were pipetted to a 96-well black polypropylene plate (Greiner Bio-One). Then, 200 μL of ethanol was added to each well and the plate was shaken in the dark for 3 h. Thereafter, the content of chlorophyll *a* was quantified by measuring the fluorescence (excitation 440 nm, emission 670 nm) with a microplate fluorometer Fluoroscan Ascent (Thermo Fischer Scientific Inc., USA). Throughout the test conditions respected the quality criteria: the algal biomass in the control cultures increased exponentially at least 16 times in the 72 h test period and the coefficient of variation did not exceed 5% throughout the experiments. The 72 h EC_{50} values (effective concentration leading to 50% reduction of biomass) were calculated as described in section 2.4.

At the end of the experiment, fluorescence micrographs were taken with Confocal Laser Scanning Microscope Zeiss-LSM-800 equipped with a digital camera to investigate the physical interactions of the algae with the nanocomposites, specifically to look for possible entrapment of algal cells in particle agglomerates and if the algal cells were still fluorescent and alive after the exposure.

2.3.4. Acute immobilization test with midge *Chironomus riparius* (OECD-235). The acute assay with *C. riparius* newborn larvae was performed following the OECD-235 guideline.¹⁷ To avoid excessive testing, only 3 representative Zn-containing materials (ZnFeZr-18:5:1 , ZnFeZr-6:1:1 and ZnFeZr-3.6:0.2:1) were selected as they already showed toxicity to *D. magna* and *R. subcapitata*. Five concentrations of the three selected nanocomposites were prepared in dechlorinated tap water with hardness ~ 400 mg L^{-1} as CaCO_3 (also used for the control and culturing of *C. riparius*): 1, 2, 5, 8 and 12 mg L^{-1} . These concentrations were chosen as the ones which were already shown to be toxic to *D. magna* and *R. subcapitata*. Newborn (<24 h) larvae were introduced into the test media in a group of 5 animals per replicate, 4 replicates per concentration ($n = 20$)

and their immobilization or mortality was monitored during 48 h. Larvae were not fed during the experiment. Testing conditions, environmental parameters (light, temperature, etc.), and test validity criteria (not more than 15% of larvae is immobilized in the control) followed the OECD-235 guidelines.¹⁷ The LC_{50} values were calculated after 24 h as described in section 2.4 (as after 48 h practically all larvae died in the treatments, though larvae in the control vessels remained viable).

2.3.5. Bacterial and algal viability assay ('Spot Test'). The 'Spot Test' was performed following the methodology by.¹⁸ It shows the ability of the toxicant-exposed bacteria *Vibrio fischeri* or algae *Raphidocelis subcapitata* to form colonies on a toxicant-free nutrient agar after 24 h exposure to the tested nanocomposites (or metal salts) in 2%NaCl (isotonic medium for marine bacteria *V. fischeri*) or in algal growth medium (ref. 13: full composition in Table S1).

Briefly, in 96-well microplates (non-tissue culture treated, BD Falcon) 100 μL of bacterial or algal suspension was added to 100 μL of varying concentrations of nanocomposite suspensions, prepared in either 2%NaCl (bacteria *V. fischeri*) or, in case of algae, in parallel in DI-water and in MOPS buffer (3-(*N*-morpholino)propanesulfonic acid); 10 mM; pH 7). Decimal dilution series of the nanocomposites in the range 1–1000 mg L^{-1} for bacteria and 1–100 mg L^{-1} for algae (nominal concentrations) were tested in triplicate.

Prior to the assay, the exponentially growing algal stock culture was washed twice with DI water *via* centrifugation (3500 g, 10 min, 25 °C). The cell density was determined by counting under a light microscope and adjusted to 1×10^6 cells per mL. Then, 100 μL algal suspension (in-test cell density 0.5×10^6 cells per mL) was added to 100 μL of varying concentrations of the nanocomposites (or metal salts).

The nanocomposite-exposed cultures were incubated for 24 h at 25 °C in the dark (bacteria) or under illumination (algae). After 24 h of exposure to the toxicants, 3 μL of the cell suspension from each microplate well was pipetted as a 'spot' onto an agarized Beneckea–Harvey (BH) growth medium for bacteria *V. fischeri* (full composition in S1) or onto agarized OECD-201 algal growth medium for *Raphidocelis subcapitata* (S2). The inoculated agar plates were incubated for several days at ~ 25 °C either in the dark (bacteria) or in constant light (algae) until the growth of colonies was visible. The *Vibrio fischeri* bioluminescent colonies were analyzed visually in the dark and photographed at 48 h.

The MBC (minimum bactericidal/biocidal concentration) of the investigated nanocomposites were determined as the lowest tested nominal concentration that completely inhibited the ability of bacteria or algae to form visible colonies after plating onto toxicant-free agar.

2.4. Statistical data analysis

All toxicity $\text{L(E)}\text{C}_{50}$ values with their respective 95% confidence intervals were calculated from dose–response curves generated with the log-normal distribution model of the REGTOX software



EV7.1.2 for Microsoft Excel™.¹⁹ The results were considered statistically significant when the 95% confidence intervals did not overlap or $p < 0.05$.

3. Results and discussion

3.1. Physico-chemical characteristics and metal solubility of the as-synthesized metal nanocomposites

The synthesis of the 2-, 3- and 4-valent metal nanocomposites followed previously published fast and simple co-precipitation procedure for layered double hydroxides (LDH) and related structures without any aging steps, air protection or complicated pH shifts, as reported in our preceding work,⁹ focusing on decreasing the amount of the potentially toxic Zn^{2+} or replacing it with other non-hazardous 2-valent metals, such as Ca^{2+} and Mg^{2+} . The chemical composition, primary particle size, surface charge (ζ -potential) and pH of the as-synthesized composites were analyzed previously⁹ and for convenience, summarized here in Table 1. Subsequently, in this study, all 11 as-synthesized materials (5 ZnFeZr-based, 5 Ca/Mg-containing and 1 magnetic ZnFeZr-6:1:1@MPs) were exposed to ecotoxicity tests to fill out the knowledge gap regarding their environmental safety.

The primary size analysis *via* laser diffraction showed that all samples had a median diameter $d_{50} = 1\text{--}10\ \mu\text{m}$ (Fig. S2). Thus, none of the composites could be considered pure nanoparticles (NPs). However, samples ZnFeZr-18:5:1, ZnFeZr-10:1:1, ZnFeZr-6:1:1 and MgZnFe-1:1:1 revealed secondary peaks $\sim 100\text{--}300\ \text{nm}$, *i.e.* presence of predominantly ZnO NPs in their structure (see XRD analysis in Fig. S3), and were analyzed further for toxicity.

In our earlier work, we tested a multitude of metal combinations in a broad variety of adsorbent materials for phosphorus removal and recovery from wastewater.⁶ We concluded that the most-promising P-adsorbent was the multi-component material ZnFeZr-6:1:1 consisting of crystalline zinc oxide nanoparticles (ZnO NPs), surrounded by amorphous zinc, iron and zirconia (oxy)hydroxides. Then, we examined the role of each constituent and found evidence that particularly the Zn-fraction and nanostructure of the material have crucial influence on the collaborative action in P-adsorption performance, indicating synergetic effects between the different components.⁷ Moreover, to facilitate harvesting of the micron-sized ZnFeZr-6:1:1 adsorbent, we deposited it on magnetic particles and the resulting magnetic adsorbent ZnFeZr-6:1:1@MPs was produced in kg-scale and successfully applied in pilot-scale tests for P-removal and recovery from wastewater.^{3,5}

Despite of the excellent P-removal and recovery performance and long-term adsorbent regeneration and reuse, dissolution of metal ions from the composite structure, particularly Zn^{2+} , was detected during the pilot test and raised concerns about the environmental safety of this promising adsorbent, since Zn is provenly toxic to many aquatic organisms, incl. bacteria, crustaceans and algae.¹¹ Indeed, preliminary solubility tests in DI water performed in our previous study⁹ and for the reader's convenience presented also in Table 2 of this follow-up work,

revealed that the most leached metal from the nanocomposites was Zn^{2+} with concentrations as high as $25.7\ \text{mg L}^{-1}$ for CaZnFeZr-3:3:1:1 (corresponds to $25.7\ \text{mg Zn per g-composite dry mass}$), $20.5\ \text{mg L}^{-1}$ for ZnFeZr-6:1:1 and $10.9\ \text{mg L}^{-1}$ for ZnFeZr-4:1:1. The lowest amount of Zn^{2+} ($0.075\ \text{mg L}^{-1}$) in DI water was leached from MgZnFe-1:1:1. Iron solubility was negligible ($Fe^{3+} \leq 0.1\ \text{mg g}^{-1}$) and zirconium was not detected ($Zr^{4+} < \text{LOD}$) in any of the samples.

3.2. Toxicity results and in-test stability of the nanocomposite suspensions

The novel nanocomposite adsorbents presented in Table 2 demonstrated high efficiency in advanced wastewater treatment for phosphorus removal and recovery from secondary effluents.^{3,5} As such, these adsorbents are meant to be applied at the final stage of the wastewater treatment process, before discharging the treated effluent into the receiving water body. Thus, it is crucial to verify their safe-by-design nature and assure environmental safety throughout their use. To gain a better understanding whether the accidental release or instability of these metal oxide/hydroxide nanocomposite adsorbent particles may pose a threat to the aquatic environment, comprehensive ecotoxicity tests were performed with several key species representative of the aqueous phase (bacteria, crustaceans, algae) and of the solid sediment phase (midge larvae). This was driven by the intrinsic properties of the nanocomposites, considering their agglomeration, rapid settling (see Fig. S4) and potential for sediment accumulation.

Table 3 summarizes the $L(E)C_{50}$ and MBC values for all nanocomposite adsorbents and all tested organisms and provides a hazard ranking assessment of the materials following a heatmap toxicity categorization described in ref. 20 and 21: $EC_{50} \leq 1\ \text{mg L}^{-1}$ = very toxic; $1 < EC_{50} \leq 10\ \text{mg L}^{-1}$ = toxic; $10 < EC_{50} \leq 100\ \text{mg L}^{-1}$ = harmful; $EC_{50} > 100\ \text{mg L}^{-1}$ = "not classified/not harmful".

At a first glance, it becomes evident that algae *R. subcapitata* and the larvae of sediment-dwelling midge *C. riparius* were the most sensitive organisms to the toxic action of all tested composites, especially to those containing Zn, with values predominantly in the red "very toxic" range: $L(E)C_{50} \leq 1\ \text{mg L}^{-1}$. The ranking is followed by crustacean *D. magna* which exhibited toxicity response only to the Zn-containing composites ($1 < EC_{50} \leq 10\ \text{mg L}^{-1}$). On the other side of the spectrum is bacterium *V. fischeri* as the least sensitive organism under the current test conditions. Similarly, only the Zn-containing composites showed inhibitory effects to *V. fischeri*, particularly those with the highest zinc-fraction (ZnFeZr-18:5:1; ZnFeZr-10:1:1) were classified as "harmful" ($10 < EC_{50} \leq 100\ \text{mg L}^{-1}$). All other composites not containing Zn were non-toxic to *Vibrio fischeri* ($EC_{50} > 100\ \text{mg L}^{-1}$, $\text{MBC} > 1000\ \text{mg L}^{-1}$). This trend is coherent with other review studies which tested a wide variety of prokaryotes (various bacteria), eukaryotes (yeast, alga, protozoa), mammalian cells *in vitro* and multicellular organisms (crustacean, fish), and also concluded that alga *R. subcapitata* is the most sensitive organism to the toxicity of



Table 3 Heatmap with toxicity end point values (L(E)C₅₀ or MBC) of all as-synthesized metal oxide/hydroxide nanocomposite adsorbents and their precursor metal salts. The listed L(E)C₅₀ values are average (minimum $n = 3$) with the respective 95% confidence intervals included in parentheses. The 24 h MBC values represent three repetitive tests ($n = 3$) with two replicates each. All concentrations are nominal: “composite-based” for the composites, and “metal-based” for the metal salts (mg Me per L)

| Test environment: | | Water | Water | Sediment | 2% NaCl solution | | |
|--|--|--|--|--|--|---|-----------------------------------|
| Test organism: | | Crustaceans <i>D. magna</i> | Algae <i>R. subcapitata</i> | Midge <i>C. riparius</i> | Bacteria <i>V. fischeri</i> | | |
| Toxicity endpoint: | | 48 h EC ₅₀ (mg L ⁻¹) | 72 h EC ₅₀ (mg L ⁻¹) | 24 h LC ₅₀ (mg L ⁻¹) | 30 min EC ₅₀ (mg L ⁻¹) | Zn-normalized 30 min EC ₅₀ (mg L ⁻¹) | 24 h MBC (mg L ⁻¹) |
| Composites | ZnFeZr-18:5:1 | 4.38 (4.06–4.83) | 0.045 (0.001–0.098) | 2.17 (1.48–8.66) | 36.9 (29.0–49.0) | 13.5 (10.6–17.9) | 100 |
| | ZnFeZr-10:1:1 | 6.48 (5.31–7.78) | 0.102 (0.049–0.113) | n.d. | 53.9 (41.0–70.0) | 20.0 (15.2–25.9) | 250 |
| | ZnFeZr-6:1:1 | 7.69 (5.59–9.88) | 0.195 (0.184–0.202) | 0.582 (0.571–0.590) | 118 (94–127) | 30.9 (24.5–33.2) | 250 |
| | ZnFeZr-6:1:1 (P-preloaded, saturated) | n.d. | 0.128 (0.113–0.167) | n.d. | n.d. | n.d. | n.d. |
| | ZnFeZr-4:1:1 | 9.01 (7.34–11.23) | 0.150 (0.132–0.164) | n.d. | 119 (105–131) | 28.7 (25.3–31.6) | 100 |
| | ZnFeZr-3.6:0.2:1 | 5.74 (4.66–7.20) | 0.103 (0.097–0.111) | 0.801 (0.395–0.913) | 168 (141–177) | 42.7 (35.8–44.9) | 250 |
| | CaFe-2:1 | >>100 | 0.317 (0.287–0.353) | n.d. | Non-toxic | Non-toxic | >1000 |
| | CaFeZr-6:1:1 | >>100 | 0.301 (0.279–0.325) | n.d. | Non-toxic | Non-toxic | >1000 |
| | CaFeZr-6:1:1 (P-preloaded, saturated) | n.d. | 0.393 (0.195–0.536) | n.d. | n.d. | n.d. | n.d. |
| | CaZnFeZr-3:3:1:1 | 12.5 (9.9–14.9) | 0.208 (0.157–0.266) | n.d. | 112 (91–118) | 20.6 (16.6–21.5) | 250 |
| | MgFeZr-6:1:1 | >>100 | 0.474 (0.424–0.539) | n.d. | Non-toxic | Non-toxic | >1000 |
| | MgFeZr-6:1:1 (P-preloaded, saturated) | n.d. | 0.416 (0.210–0.577) | n.d. | n.d. | n.d. | n.d. |
| | MgZnFe-1:1:1 | >100 | 0.222 (0.197–0.252) | n.d. | 486 (391–598) | 81.4 (65.5–99.9) | >1000 |
| | ZnFeZr-6:1:1@MPs | >>100 | 3.81 (3.31–4.39) | n.d. | 1123 (929–1173) | 58.8 (48.6–61.4) | >1000 |
| | ZnFeZr-6:1:1@MPs (P-preloaded, saturated) | n.d. | 4.54 (3.65–5.31) | n.d. | n.d. | n.d. | n.d. |
| Precursor metal salts | ZnCl ₂ | 1.40 ^a | 0.114 (0.103–0.123) | >25.0 ^a | 17.5 (14.4–18.9) | | 50.0 |
| | CaCl ₂ ·2H ₂ O | n.d. | n.d. | n.d. | Non-toxic | | >1000 |
| | MgCl ₂ ·6H ₂ O | n.d. | n.d. | n.d. | Non-toxic | | >1000 |
| Very toxic EC ₅₀ ≤ 1 mg L ⁻¹ | Toxic 1 < EC ₅₀ ≤ 10 mg L ⁻¹ | | Harmful 10 < EC ₅₀ ≤ 100 mg L ⁻¹ | | Not classified/not harmful EC ₅₀ > 100 mg L ⁻¹ | | |

Remarks: the results on bacteria *V. fischeri* are adopted from ref. 9. L(E)C₅₀: half-lethal/effective concentration 50%; MBC: minimum bactericidal concentration. Hazard ranking and color-coding based on ecotoxicity classification as described in ref. 20. n.d. – “not determined”; n.a. – “not applicable”. ^a L(E)C₅₀ values are taken from Table S5.

ZnO NPs and soluble Zn-salt.^{11,21} Further investigations for each tested organism and potential toxicity mechanisms are discussed in the following sub-sections.

3.2.1. Toxicity to bacteria *Vibrio fischeri*. As noted above, all toxicity test results concerning bacteria *Vibrio fischeri* are taken from our previous paper⁹ and are summarized here for comparison and completeness of this study.

The Gram-negative bioluminescent marine bacterium *V. fischeri* was used as a model organism for rapid initial ecotoxicity screening of the studied nanocomposites due to its quick response to various toxicants (including turbid and colorful samples like the tested chemicals), leading to

decrease in bioluminescence proportional to the toxicity of the chemical.

The performed 30 min kinetic bioluminescence inhibition test (standard protocol ISO-21338:2010, ‘Flash Assay’) resulted in nanocomposite-specific 30 min EC₅₀ values, summarized in Table 3. Bioluminescence inhibition is a sub-lethal response which correlated well with the bacterial viability/mortality endpoint after 24 h extended exposure to the nanocomposites, expressed as 24 h MBC values (Table 3). To define MBC, viability assay (‘Spot Test’) was also performed and for reader’s convenience results are included in Fig. S5.



All nanocomposites settled rapidly in the test medium (2% NaCl) due to their μm -sized particles ($d_{50} = 1\text{--}10 \mu\text{m}$), which may influence their toxicity by reducing interactions with the test bacteria. Thus, soluble Zn^{2+} ions leached from the nanocomposites became a key factor as potential cause for toxicity. Furthermore, heteroaggregation effects causing bacterial cell entrapment by the nanocomposites²² may also not be excluded as an experimental artefact which influences the toxicity of nanomaterials.²³ This was, for instance, the case for green algae *R. subcapitata*, discussed later in section 3.2.3, for which entrapment in particle agglomerates caused inhibition of growth, although captured algal cells were still alive (based on fluorescence). However, the observed responses by bacteria *V. fischeri* in this study are unlikely to be driven by heteroaggregation. The endpoint for the performed *V. fischeri* assay (ISO-21338:2010) was inhibition of bioluminescence and not inhibition of growth, which reflects disruption of the cellular metabolic activity, and not the ability of cells to grow. To avoid such potential artefacts, a ‘Spot Test’ (viability assay) was also conducted as an additional toxicity endpoint for the *V. fischeri* luminescence inhibition results. In contrast to algae, effects toward *V. fischeri* were observed only for the Zn-containing materials, which is consistent with Zn ion-driven effects rather than aggregation-related growth limitations, as supported by the results from both bioluminescence inhibition assay (Table 3) and viability-based ‘Spot Test’ (Fig. S5).

Hazard ranking based on EC_{50} -values showed increasing toxicity with higher Zn content in the composites. The materials with highest Zn-fraction ZnFeZr-18:5:1 and ZnFeZr-10:1:1 were classified as “harmful” ($10 < \text{EC}_{50} \leq 100 \text{ mg L}^{-1}$), likely due to the presence of ZnO nanoparticles in their structure and leached Zn^{2+} . All Zn-containing compounds fell either in the “harmful” range or close to it with $\text{EC}_{50} \sim 100 \text{ mg L}^{-1}$. Only MgZnFe-1:1:1 was “not harmful” ($\text{EC}_{50} = 486 \text{ mg L}^{-1}$), attributed to low Zn^{2+} solubility (Table 2). This correlated well with the lethal endpoint from ‘Spot Test’ with 24 h MBC $\leq 250 \text{ mg L}^{-1}$ for all Zn-containing composites, except for MgZnFe-1:1:1 with 24 h MBC $> 1000 \text{ mg L}^{-1}$.

All other nanocomposites without Zn in their structure, regardless of their composition, were non-toxic to *Vibrio fischeri* even at the highest tested concentration (24 h MBC $> 1000 \text{ mg L}^{-1}$). This confirms the assumption that the acute toxicity effects were attributed only to the presence of Zn^{2+} ions and ZnO (nano)particles. The high toxicity of bioavailable Zn^{2+} ions and ZnO (both bulk and nano-sized) to *Vibrio fischeri* was reported by others as well with 30 min $\text{EC}_{50} = 1.8\text{--}11.5 \text{ mg L}^{-1}$.¹⁶

Furthermore, all Zn-based composites were positively charged at neutral pH with ζ -potential from +8.3 to +27.7 mV (see Table 1) inferring their strong electrostatic attraction to the negatively charged *Vibrio fischeri* cell membrane (ζ -potential -21.8 mV) causing inhibition of bioluminescence via disruption of the cell membrane integrity.

These results of pre-screening for ecotoxicity with *Vibrio fischeri* showed that the luminescent bacteria were sensitive only

to the Zn-containing compounds, which motivated us to perform 3 additional bioassays with more sensitive organisms discussed in the following sub-sections.

3.2.2. Toxicity to crustacean *Daphnia magna*. Crustaceans play an important role in the aquatic ecosystem as primary and secondary consumers. Freshwater crustacean *Daphnia magna* is a model organism recommended for chemical safety assessment under the REACH regulation.¹²

The acute toxicity tests in this work assess the short-term effect of each nanocomposite on *Daphnia magna* over a 48 h exposure period using immobilization of the test organisms as an endpoint, quantified through EC_{50} values obtained from dose–response curves and summarized in Table 3. In contrast to bacteria *V. fischeri*, the crustaceans were more sensitive to the Zn-containing composites which were all toxic to *D. magna* ($1 < \text{EC}_{50} \leq 10 \text{ mg L}^{-1}$). Exceptionally, only CaZnFeZr-3:3:1:1 was “harmful” ($\text{EC}_{50} = 12.5 \text{ mg L}^{-1}$) and MgZnFe-1:1:1 was classified as “not harmful” ($\text{EC}_{50} > 100 \text{ mg L}^{-1}$). The lack of acute toxicity of the latter MgZnFe-1:1:1 could be attributed to higher stability (ζ -potential = 27.7 mV, Table 1) and lowest leaching of soluble Zn^{2+} (0.075 mg g^{-1}) among all other Zn-containing composites in DI water (Table 2) and in *D. magna* OECD-202 test medium (Fig. 1).

Generally, all composites settled quickly (within 30 min) at the bottom of the test wells (see Fig. S6 in SI) due to their μm -ranged primary particle size ($d_{50} > 3 \mu\text{m}$, Table 1). Nevertheless, at the end of the test after 48 h, Zn was detected in the water column of all exposure concentrations of the Zn-containing composites (Fig. 1, grey bars) due to the presence of leached bioavailable Zn^{2+} ions, as well as suspended colloidal Zn-based (nano)particles. The samples were collected from the upper layer of the water column, avoiding re-suspension of the settled nanocomposites. Total Zn consists of Zn ions and colloidal NPs. Full metal solubility analysis is included in the SI, showing the total metal concentrations in all well-homogenized exposure particle concentrations in the beginning of the test (Table S2), and the total metal concentrations in the clear water columns at the end of the static tests (Tables S3 and S4).

Previous research has shown that the ZnFeZr-based adsorbents consist of crystalline ZnO nanoparticles (NPs) surrounded by amorphous (oxy)hydroxides of Zn, Fe and Zr.⁷ Other studies demonstrated that the toxicity of ZnO NPs is associated mainly with the dissolution of Zn^{2+} ions.²⁴

The results in Fig. 1 do not show a strong correlation between the nominal exposure concentration (3.125–100 mg L^{-1} ; referring to the whole composite) and the Zn concentration in the water column (grey bars) after 48 h. Higher test concentrations did not necessarily lead to higher Zn concentration in the water column. Nevertheless, the highest 48 h immobilization effect in % (Fig. 1, red circles) was observed at the highest nominal exposure concentration (100 mg L^{-1}) for majority of the Zn-containing composites, or alternatively at the second highest exposure concentration (50 mg L^{-1}) for ZnFeZr-3.6:0.2:1, CaZnFeZr-3:3:1:1 and MgZnFe-1:1:1.



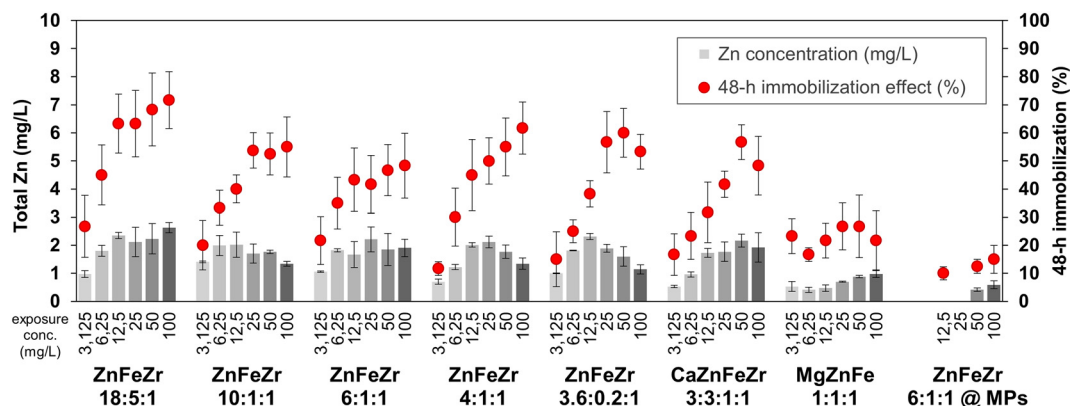


Fig. 1 Immobilization effect (%) on *Daphnia magna* (red circles, right Y-axis) after 48 h of exposure to different concentrations of the nanocomposites (3.1–100 mg L⁻¹) and associated total Zn concentrations (mg L⁻¹) in the supernatants (grey bars, left Y-axis) collected from the water column of each exposure concentration ($n = 3$) at the end of the test. Remark: the plotted data refers only to the Zn-containing nanocomposites.

Among all Zn-containing nanocomposites, the lowest acute immobilization effect (<20%) was observed for the magnetic adsorbent ZnFeZr-6:1:1@MPs (Fig. 1), which was not harmful to *D. magna* ($EC_{50} \gg 100 \text{ mg L}^{-1}$, Table 3), unlike its non-magnetic version ZnFeZr-6:1:1 which was toxic ($EC_{50} = 7.7 \text{ mg L}^{-1}$). This indicates that, once deposited onto magnetic particles, the composite adsorbent ZnFeZr-6:1:1@MPs was rather stable and caused low immobilization effect (<20%) even at the highest test concentration of 100 mg L^{-1} (Fig. 1). Similar conclusions were drawn for bacteria *V. fischeri* with 24 h MBC = 250 mg L^{-1} for the adsorbent ZnFeZr-6:1:1 versus 24 h MBC > 1000 mg L^{-1} for the magnetic version of the same adsorbent ZnFeZr-6:1:1@MPs (Table 3). The better stability and lower toxicity of ZnFeZr-6:1:1@MPs was mainly due to the lower zinc fraction (5.2 wt%, Table 1), as 80 wt% of the molar mass was the magnetite-silica core serving as magnetic carrier in the composite micro-particles. Furthermore, the magnetic composite ZnFeZr-6:1:1@MPs had a significantly larger primary particle size (>20 μm , Table 1). It is well-known that the particle size influences the particle solubility and toxic potency and affects the way microcrustaceans interact with the particles.^{25,26}

Regarding Zn-ions and nano-ZnO, the acute toxicity EC_{50} -values reported in literature for *D. magna* vary in the range 1.4–3.1 mgZn per L and was caused mainly by solubilized Zn-ions (see Table S5), which is in agreement with the Zn-normalized EC_{50} values for all nanocomposites in this study: 1.4–2.4 mgZn per L (Table S6). Table S5 compares literature data on $L(E)C_{50}$ -values for *Daphnia magna*, *Vibrio fischeri*, *Raphidocelis subcapitata* and *Chironomus riparius* regarding the five metals (Zn, Fe, Zr, Ca, Mg) relevant for this work.

The most toxic metal for the majority of test organisms was Zn ($1 < EC_{50} \leq 10 \text{ mg L}^{-1}$) and, similar to our findings, other studies also concluded that *D. magna* is more sensitive than *V. fischeri* to Zn-containing compounds. All other composites without Zn were not toxic to *D. magna* ($EC_{50} \gg 100 \text{ mg L}^{-1}$, Table 3), which aligns with the literature data in Table S5 (Ca, Mg and Zr had $EC_{50} \gg 100 \text{ mg L}^{-1}$). This leads to the conclusion that toxicity was caused

primarily by the presence of Zn in the materials' structure, particularly by the leaching of Zn^{2+} ions.

However, microcrustaceans are particle-ingesting species which can uptake soluble metals either directly from water through their body surface or from the ingested particles. *Daphnia* may ingest suspended particles up to 70 μm in size.²⁷ Furthermore, the mechanical adhesion of nanoparticles on the organism surface of microcrustaceans can cause various negative effects such as molting problems due to inhibition of gene expressions related to molting and energy metabolism.²⁸ This is a concern for some of the tested materials like ZnFeZr-18:5:1 and ZnFeZr-10:1:1 which contained ZnO nanoparticles in their structure (see Fig. S2 and S3).

After the acute test, exposed *Daphnia magna* specimens were analyzed microscopically to investigate further how the test organisms interacted with the nanocomposites. The findings suggest that the distress experienced by *D. magna* cannot be attributed solely to soluble Zn^{2+} . For example, Fig. 1 shows that at the highest test concentration 100 mg L^{-1} , materials ZnFeZr-6:1:1 and CaZnFeZr-3:3:1:1 leached more soluble Zn than materials ZnFeZr-10:1:1, ZnFeZr-4:1:1 and ZnFeZr-3.6:0.2:1 but, counterintuitively, the first two exhibited lower immobilization effect on *D. magna*, possibly due to their higher hydrodynamic particle size ($D_h > 1000 \text{ nm}$) reported in our previous work.⁹ In contrast, the hydrodynamic size of ZnFeZr-10:1:1, ZnFeZr-4:1:1 and ZnFeZr-3.6:0.2:1 was much lower ($D_h = 376\text{--}716 \text{ nm}$), which facilitated easy ingestion of the particles by the microcrustaceans. Indeed, the microscopic images in Fig. 2 reveal ingested nanocomposite particles ZnFeZr-10:1:1 in the gut of *D. magna* (Fig. 2b), as well as particle adhesion on the exoskeleton of the microcrustaceans and particle agglomerates causing immobilization of *D. magna* (Fig. 2c and d). Also, the non-toxic CaFe-2:1 was ingested by *Daphnia* (Fig. 2c), although it proved to be “not harmful” ($EC_{50} > 100 \text{ mg L}^{-1}$) due to the lack of Zn in its composition.

3.2.3. Toxicity to green algae *Raphidocelis subcapitata*. The green freshwater microalgae *Raphidocelis subcapitata* (formerly *Pseudokirchneriella subcapitata*) is a model organism for aquatic



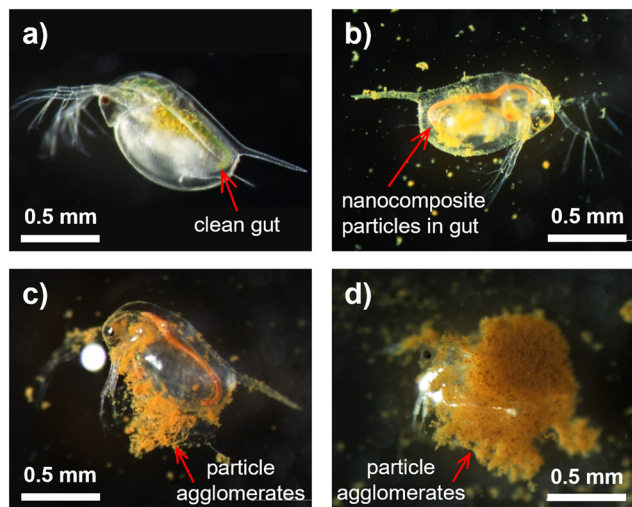


Fig. 2 Light microscopy images of crustacean *Daphnia magna* in OECD-202 medium after 48 h exposure to: a) not exposed (control); b) 50 mg L⁻¹ ZnFeZr-10:1:1 indicating ingestion of nanocomposite particles in the gut of *Daphnia*; c) 100 mg L⁻¹ CaFe-2:1 and d) 100 mg L⁻¹ ZnFeZr-6:1:1@MPs showing particle agglomerates causing immobilization of *Daphnia*.

toxicity with high sensitivity to various toxicants. Algae *R. subcapitata* are unicellular organisms representing a base trophic level in the aquatic food chain as primary producers which are very sensitive, especially to heavy metals. Indeed, heavy metals like zinc are highly toxic to algae already at $\mu\text{g L}^{-1}$ level.¹¹ Algae have a short generation time allowing for rapid detection of adverse effects over several generations within just 72 h exposure time.

Considering that only the Zn-containing compounds were toxic to bacteria and crustaceans, first we studied the dissolution of Zn²⁺ ions in the algal medium¹³ at the end of the 72 h exposure as the most probable mechanism of direct toxicity to algae. The results plotted in Fig. 3 show similar trends as in *D. magna* medium (Fig. 1). Namely, the highest Zn dissolution (2.1 mg Zn per L) occurred in the materials with highest Zn-fraction ZnFeZr-18:5:1 and ZnFeZr-3.6:0.2:1, whereas lowest Zn dissolution (0.2 mg Zn per L) was observed for materials ZnFeZr-6:1:1@MPs and MgZnFe-1:1:1, similar to the *Daphnia* tests. Furthermore, the Zn solubility in both OECD media (Fig. 1 and 3) was lower than in DI water (Table 2) which is in agreement with other researchers' findings.²⁹

Nevertheless, the toxicity heatmap in Table 3 shows indisputably that all adsorbents (even those without Zn) were very toxic to algae ($\text{EC}_{50} \leq 1 \text{ mg L}^{-1}$), except for ZnFeZr-6:1:1@MPs with higher EC_{50} value but still toxic ($1 < \text{EC}_{50} \leq 10 \text{ mg L}^{-1}$). This infers that besides the "direct" toxicity caused by dissolution of Zn²⁺ ions, there must be another mechanism of "indirect" toxicity, e.g. through nutrients removal from the medium. Indeed, all studied nanocomposites were originally designed to remove phosphate from wastewater, which is a critical nutrient for algal growth. Moreover, Gao *et al.* revealed that zinc toxicity to alga *Pseudokirchneriella subcapitata* decreased under phosphate limiting growth conditions.³⁰

To address this problem, 4 selected materials – 2 with Zn (ZnFeZr-6:1:1; ZnFeZr-6:1:1@MPs) and 2 without Zn (CaFeZr-6:1:1; MgFeZr-6:1:1) – were preloaded with phosphate until saturation and fully exhausted adsorption capacity, *i.e.* until they could not adsorb phosphate anymore (details included in

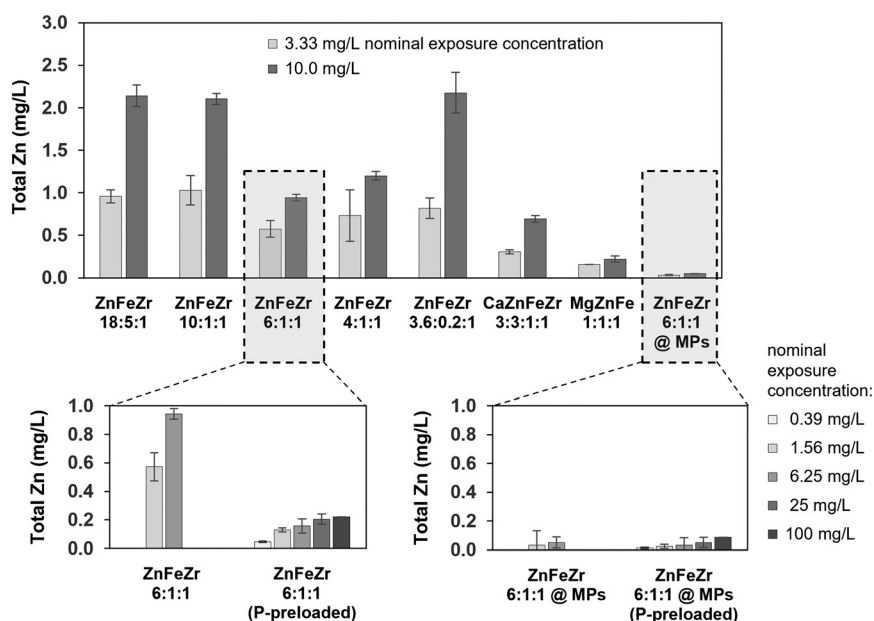


Fig. 3 Total Zn concentration (mg L^{-1}) measured with TXRF in the filtered supernatants collected from the water column ($n = 3$) of the tests with algae *Raphidocelis subcapitata* after 72 h exposure to the nanocomposite particles at various exposure concentrations. Remark: the plotted data refers only to the Zn-containing nanocomposites.



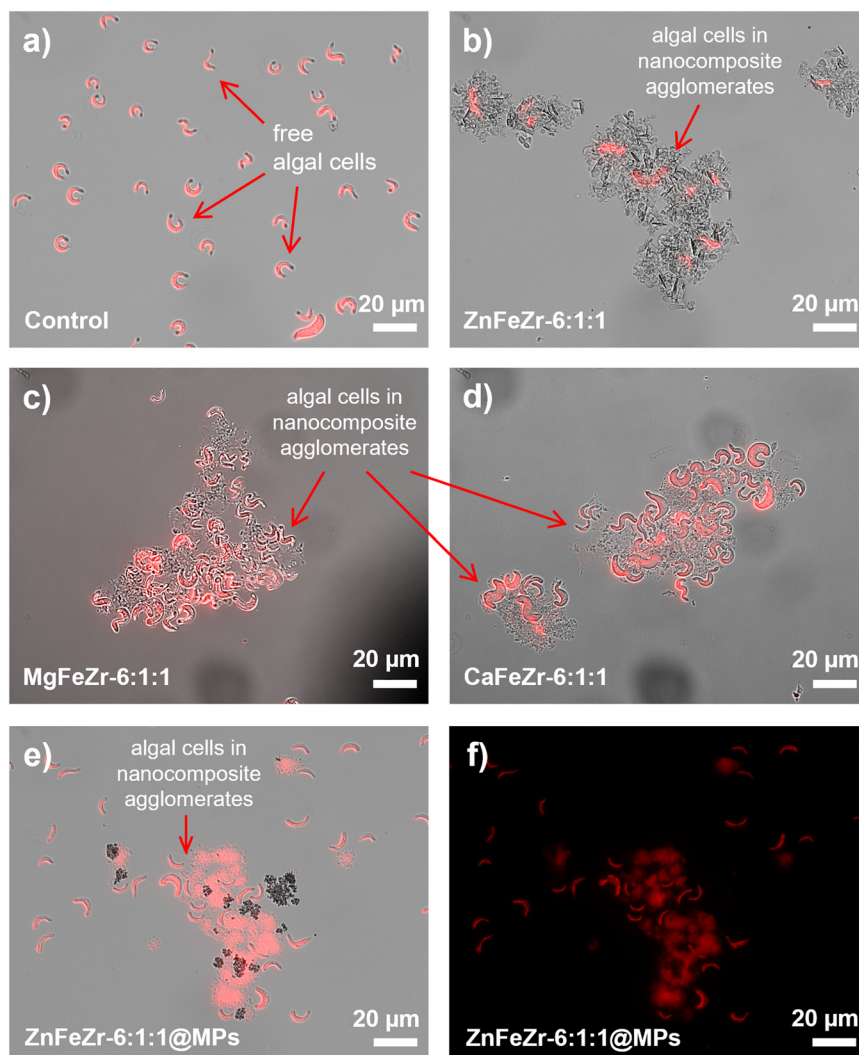


Fig. 4 Fluorescence microscopy images of algae *Raphidocelis subcapitata* captured in particle agglomerates after 72 h exposure to P-preloaded adsorbents: a) not exposed (control, pure algae); b) 1 mg L^{-1} ZnFeZr-6:1:1; c) 1 mg L^{-1} MgFeZr-6:1:1; d) 1 mg L^{-1} CaFeZr-6:1:1, and e) 5 mg L^{-1} ZnFeZr-6:1:1@MPs photographed in parallel using overlay of differential interference contrast (DIC) with fluorescent image and f) only fluorescence microscopy. Remark: images a)–e) represent an overlay of DIC with fluorescence microscopy performed with a confocal laser scanning microscope Zeiss-LSM-800.

S3). Subsequently, these 4 P-preloaded materials were also subjected to the algae toxicity assay.

The lower panel inserts in Fig. 3 verify that the soluble Zn-concentration in the filtered supernatants of the P-preloaded materials was lower than in their non-preloaded counterparts, assumingly due to binding interactions between the free zinc on the adsorbents surface and the phosphate ions in solution, leading to formation of insoluble $\text{Zn}_3(\text{PO}_4)_2$ and inner-sphere surface ligand complexes.^{5,7} Thus, it was intuitively expected that the P-preloaded materials would be less toxic to algae due to significantly reduced leaching of soluble Zn (especially in case of ZnFeZr-6:1:1, Fig. 3 bottom left) and inability to uptake phosphate from the algal growth medium, but this was not the case. Table 3 shows that all P-preloaded materials, irrespective of whether they contain Zn or not, were all very toxic to algae ($\text{EC}_{50} \leq 1 \text{ mg L}^{-1}$), meaning that algal growth inhibition

involves other mechanisms beyond soluble Zn^{2+} and nutrients uptake from the medium.

To elucidate this issue, further microscopic investigations revealed that all nanocomposites (including the P-preloaded ones) formed agglomerates entrapping algal cells which precipitated at the bottom of the vials and were even visible with a naked eye at test concentrations $\geq 1 \text{ mg L}^{-1}$. The microscopic images in Fig. 4b–f demonstrate this effect of algal cells captured into particle agglomerates for all four P-preloaded adsorbents, including the magnetic ZnFeZr-6:1:1@MPs (Fig. 4e and f) which had an order-of-magnitude higher EC_{50} value ($\text{EC}_{50} = 4.54 \text{ mg L}^{-1}$) but still was classified as toxic. For comparison, Fig. 4a shows pure free algal cells (control, not exposed to toxicants) still homogeneously distributed in OECD-201 medium after 72 h of undisturbed exponential growth. This verifies the hypothesis that particle agglomerates cause



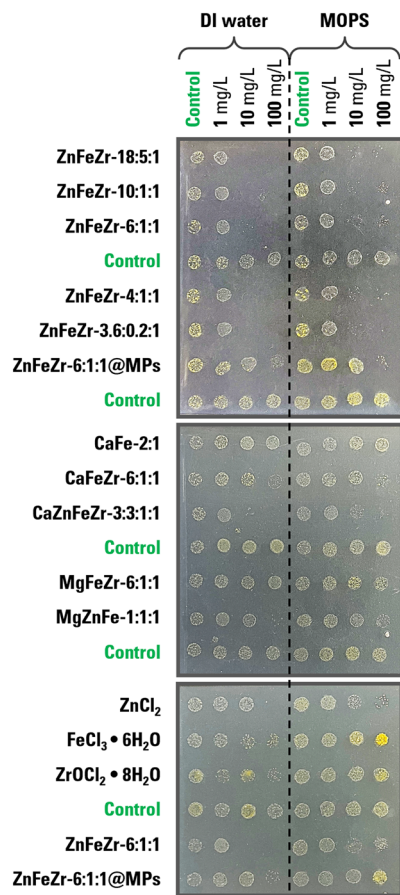


Fig. 5 Colony-forming ability of algae *Raphidocelis subcapitata* on agar after 24 h exposure to the 11 metal oxide/hydroxide nanocomposite adsorbents and their precursor metal salts in deionized (DI) water and in MOPS buffer. Remark: all concentrations are nominal and refer to “mg-compound/L”.

inhibition of algal growth through physical entrapment of algal cells, which may also block access to light and nutrients, hinder their metabolism and increase exposure to bioavailable dissolved metal ions in the vicinity of the aggregates. Nevertheless, the entrapped algal cells themselves remained intact and were still viable inside the agglomerates (confirmed by their continuous fluorescence), but the algal biomass did not increase over the 72 h incubation. Similar particle agglomeration effects were reported by others as a common algal toxicity mechanism.^{21,29}

To understand better the toxicity mechanisms, additional ‘Spot Test’ was performed following the methodology described in ref. 18. The advantage of this test is that it avoids the effect of indirect toxicity through nutrients removal from the medium as algae were exposed to the substances for 24 h in pure deionized (DI) water or in MOPS buffer without any nutrients and subsequently incubated on a toxicant-free nutrient agar. Despite the hypotonic conditions of DI water, the strong cell wall of *R. subcapitata* keeps the algae viable throughout the 24 h test period,²⁹ as confirmed by the healthy growth in all “Control” series (Fig. 5, green font). In parallel with the nanocomposites,

their precursor metal salts were tested as well. Since DI water has pH ~5.5 and the precursor salts $\text{FeCl}_3 \cdot 6\text{H}_2\text{O}$ and $\text{ZrOCl}_2 \cdot 8\text{H}_2\text{O}$ had in test pH 3–5.5, outside the recommended testing range for *R. subcapitata* (pH 7.5–8.1), all experiments were performed in parallel also in MOPS buffer (pH 7).

The ‘Spot Test’ results in Fig. 5 show that for all Zn-containing nanocomposites the minimum biocidal concentration (MBC) could be identified at 10 mg L^{-1} , at which the algal cells were not able to grow anymore on nutrient agar. The two exceptions were MgZnFe-1:1:1 and the magnetic ZnFeZr-6:1:1@MPs still showing some poor growth even at 100 mg L^{-1} , which correlates well with the low Zn solubility of both materials (Fig. 3) and with the higher EC_{50} -values in Table 3. Furthermore, the MBC-values were at least one order-of-magnitude higher than the EC_{50} -values which can be explained with the different sensitivity of the endpoints, namely inhibition of growth versus mortality, and with the different exposure time, which was longer and under constant shaking in the case of the 72 h algal growth inhibition assay.

The colony forming potency of toxicants-exposed algae in MOPS was not significantly higher than in DI water, implying that the adverse effects were not due to unfavorable pH. Even when accounting for pH and nutrients removal disturbances, the inhibitory effect remained among all Zn-containing materials, meaning that the presence of soluble Zn^{2+} is one of the main toxicity mechanisms. In contrast, the materials without Zn (CaFe-2:1 ; CaFeZr-6:1:1 ; MgFeZr-6:1:1) did not hinder the algal colony-forming ability even at 100 mg L^{-1} , inferring that in their case the inhibition of growth in the 72 h test was rather caused by agglomeration effects and nutrients uptake.

Overall, the toxicity of all nanocomposites was more pronounced in the 72 h growth inhibition assay (Table 3) than in the ‘Spot Test’ (Fig. 5). It must be noted that the ‘Spot Test’ yielded rather rough estimate of toxicity, as decimal dilutions of the compounds were used ($1, 10, 100 \text{ mg L}^{-1}$) to cover a larger concentration range. Furthermore, the physico-chemical properties of the natural receiving water body may increase or decrease the bioavailability of the toxicants, which is especially important when studying the chronic toxicity effects to freshwater organisms. Parameters such as pH and temperature may increase the solubilization and bioavailability of toxic metal ions, as confirmed by the ‘Spot Test’ where toxicity of the precursor metal salts ZnCl_2 , $\text{FeCl}_3 \cdot 6\text{H}_2\text{O}$ and $\text{ZrOCl}_2 \cdot 8\text{H}_2\text{O}$ (Fig. 5, bottom panel) was more evident in slightly acidic DI water and less apparent at neutral pH in the MOPS buffer. On the other hand, the presence of organic matter/humic substances, suspended solids and high salinity may lead to agglomeration and sedimentation of potentially harmful nanoparticles, respectively decrease their bioavailability and toxicity. However, it has also been shown that natural organic matter (NOM) interacts strongly with nanoparticles, modifying their surfaces and that NOM could also stabilize colloidal particles through the combining effects of charge neutralization and steric hindrance, thus retarding the nanoparticle suspension



due to bridging forces³¹ and preventing heteroagglomeration effects with aquatic microorganisms.

3.2.4. Toxicity to sediment-dwelling midge *Chironomus riparius*. The goal of this acute bioassay with midge *C. riparius* larvae was to compare the response of this sediment-dwelling organism with that of the aquatic species *V. fischeri*, *D. magna* and *R. subcapitata*. To avoid excessive testing, only 3 representative Zn-containing materials (ZnFeZr-18:5:1, ZnFeZr-6:1:1 and ZnFeZr-3.6:0.2:1) were selected as they already showed toxicity to *D. magna* and *R. subcapitata* (Table 3).

The 24 h LC₅₀ data showed that all 3 tested composites were acutely “toxic” to “very toxic” to newborn *C. riparius* larvae. As low as 0.57–0.80 mg L⁻¹ of tested compounds caused 50% mortality ($n = 20$) (Table 3). The international aquatic life quality guidelines for dissolved Zn concentrations in freshwaters indicate acute toxicity at 120 µg L⁻¹ (ref. 32) and from 90–400 µg L⁻¹ depending on water hardness.³³ As the toxicity of Zn-ions towards *C. riparius* was relatively low for soft water (>25 mg L⁻¹; Table 3), the shed Zn-ions from the Zn-containing nanocomposites (Table 2) could not be the cause of their high toxicity to midges. The higher toxicity observed with the tested nanocomposites may be attributed to the bioavailable intracellular Zn levels which are caused by Zn-based nanoparticles. The XRD diffractograms of the tested nanocomposites (Fig. S3) showed that ZnFeZr-18:5:1 and ZnFeZr-3.6:0.2:1 contain nanoparticles in the form of Zn-oxides (ZnO and Zn(OH)₂, respectively). Nanoparticles of ZnO (30 nm, 100 mg L⁻¹) were internalized by mammalian immune cells after 24 h exposure where they dissolved into bioavailable Zn and generated oxidative stress, reducing the cell viability to 20%.³⁴ Fast precipitation of the tested nanocomposites (within 30 min, Fig. S4) may stimulate nanoparticle contact with the *C. riparius* larvae which tend to find any substrate to attach to soon after hatching. The direct cytotoxic effect of Zn nanoparticles after uptake by *C. riparius* larvae (either through skin or by ingestion) could also be a reason for the lower survival rates of these sediment-dwelling organisms, compared to aqueous *D. magna* (Table 3).

4. Conclusions

This work provided a comprehensive environmental safety assessment of 11 novel nanocomposite adsorbents using 4 different aquatic organisms, which advances the material commercialization in line with the “Safe-and-Sustainable-by-Design” principle.

Stability tests showed that all Zn-containing materials leached potentially toxic Zn²⁺ ions in all test media, even after reducing the share of Zn in the composites. Moreover, the composites with highest Zn-fraction (ZnFeZr-18:5:1, ZnFeZr-10:1:1) revealed also presence of hazardous ZnO nanoparticles. Thus, according to the data obtained with acute toxicity tests, all Zn-containing materials were indisputably “harmful” ($10 < EC_{50} < 100$ mg L⁻¹) to bacteria *Vibrio fischeri*, “toxic” ($1 < EC_{50} < 10$ mg L⁻¹) to crustacean *Daphnia magna* and “very toxic” ($L(E)C_{50} < 1$ mg L⁻¹) to algae

Raphidocelis subcapitata and the larvae of midge *Chironomus riparius*. The rest of the composites that were not containing Zn proved non-toxic to *V. fischeri* and *D. magna* but were still very toxic to algae *R. subcapitata*.

Once deposited onto magnetic particles, the pilot-scale tested material ZnFeZr-6:1:1@MPs was rather stable and did not show any acute toxicity effects neither to *V. fischeri* (30 min EC₅₀ > 1000 mg L⁻¹; 24 h MBC > 1000 mg L⁻¹) nor to *D. magna* (48 h EC₅₀ >> 100 mg L⁻¹), but it still remained quite “toxic” to algae *R. subcapitata* ($1 < 72$ h EC₅₀ < 10 mg L⁻¹).

From an engineering perspective, this means that only the application of Zn-free composites should be safe for the aquatic environment, and only if the adsorbent harvesting and separation process is well-secured within the controlled engineering facility. Realistic adsorbent concentrations for engineering applications are in the range 200–1000 mg L⁻¹, depending on the phosphate concentration in wastewater, which may cause adsorbent-induced acute toxicity effects. Therefore, it is not recommended to apply the Zn-containing adsorbents directly in the WWTP biological treatment step, as this may also inhibit the activated sludge biomass, but as a separate step after the biological pre-treatment of the wastewater. However, it should be considered that if a material is classified “toxic” due to *e.g.* physical entrapment of microorganisms in particle aggregates tested under controlled laboratory conditions, it does not necessarily mean that this can be extrapolated to a real environmental setting where many other factors (natural organic matter, pH, temperature, *etc.*) play a role and often times reduce the toxicity by *e.g.* keeping colloidal nanocomposite particles in suspension and preventing heteroaggregation effects. Therefore, for complete risk assessment analysis, further research is needed on realistic environmental exposure scenarios and more inclusive ecotoxicity tests, including investigation of chronic effects.

Conflicts of interest

There are no conflicts of interest to declare.

Data availability

The data supporting this article have been included as part of the supplementary information (SI).

Supplementary information: the SI file includes additional methods description of the *Vibrio fischeri* tests and the phosphate preloading of the adsorbents, as well as figures and tables related to the characterization of the nanocomposites, *V. fischeri* ‘Spot Test’ results and comparison literature data on L(E)C₅₀ values for all tested organisms. See DOI: <https://doi.org/10.1039/d5en00887e>.

Acknowledgements

Asya Drenkova-Tuhtan acknowledges the European Commission for the individual fellowship (Grant agreement ID:



867457, Project “NanoPhosTox”) within the Marie Skłodowska-Curie MSCA-IF-EF-ST funding scheme of the European Union’s Horizon 2020 research and innovation programme H2020-EU.4 (spreading excellence and widening participation). Irina Blinova acknowledges grant PRG1427 and Anne Kahru grant PRG2595 from the Estonian Research Council. We thank gratefully Olha Alieksieva, Heiki Vija, Maarja Otsus, Triin Vaimann and Kevin Uke for the invaluable laboratory assistance.

References

- 1 EU Commission, *Directive (EU) 2024/3019 of the European Parliament and of the Council of 27 November 2024 concerning urban wastewater treatment (recast)*, 2024.
- 2 P. Loganathan, S. Vigneswaran, J. Kandasamy and N. S. Bolan, Removal and recovery of phosphate from water using sorption, *Crit. Rev. Environ. Sci. Technol.*, 2014, **44**, 847–907, DOI: [10.1080/10643389.2012.741311](https://doi.org/10.1080/10643389.2012.741311).
- 3 A. Drenkova-Tuhtan, E. K. Sheeleigh, E. Rott, C. Meyer and D. L. Sedlak, Sorption of recalcitrant phosphonates in reverse osmosis concentrates and wastewater effluents – influence of metal ions, *Water Sci. Technol.*, 2021, **83**, 934–947, DOI: [10.2166/wst.2021.026](https://doi.org/10.2166/wst.2021.026).
- 4 E. Rott, M. Nouri, C. Meyer, R. Minke, M. Schneider, K. Mandel and A. Drenkova-Tuhtan, Removal of phosphonates from synthetic and industrial wastewater with reusable magnetic adsorbent particles, *Water Res.*, 2018, **145**, 608–617, DOI: [10.1016/j.watres.2018.08.067](https://doi.org/10.1016/j.watres.2018.08.067).
- 5 A. Drenkova-Tuhtan, M. Schneider, M. Franzreb, C. Meyer, C. Gellermann and G. Sextl, *et al.* Pilot-scale removal and recovery of dissolved phosphate from secondary wastewater effluents with reusable ZnFeZr adsorbent@Fe₃O₄/SiO₂ particles with magnetic harvesting, *Water Res.*, 2017, **109**, 77–87, DOI: [10.1016/j.watres.2016.11.039](https://doi.org/10.1016/j.watres.2016.11.039).
- 6 A. Drenkova-Tuhtan, M. Schneider, K. Mandel, C. Meyer, C. Gellermann, G. Sextl and H. Steinmetz, Influence of cation building blocks of metal hydroxide precipitates on their adsorption and desorption capacity for phosphate in wastewater—A screening study, *Colloids Surf., A*, 2016, **488**, 145–153, DOI: [10.1016/j.colsurfa.2015.10.017](https://doi.org/10.1016/j.colsurfa.2015.10.017).
- 7 M. Schneider, A. Drenkova-Tuhtan, W. Szczerba, C. Gellermann, C. Meyer and H. Steinmetz, *et al.* Nanostructured ZnFeZr oxyhydroxide precipitate as efficient phosphate adsorber in waste water: understanding the role of different material-building-blocks, *Environ. Sci.: Nano*, 2017, **4**, 180–190, DOI: [10.1039/C6EN00507A](https://doi.org/10.1039/C6EN00507A).
- 8 M. Cwieneczek and R. Ulber, Magnetic separation for sustainable phosphorus recovery: Advances, challenges, and future perspectives, *J. Water Process Eng.*, 2026, **82**, 109497, DOI: [10.1016/j.jwpe.2026.109497](https://doi.org/10.1016/j.jwpe.2026.109497).
- 9 A. Drenkova-Tuhtan, M. Sihtmäe, K. Uke, H. Vija, M. Oppmann and J. Prieschl, *et al.* Synthesis and ecotoxicity screening of reusable, magnetically harvestable metal oxide/hydroxide nanocomposites for safe and sustainable removal and recovery of phosphorus from wastewater, *J. Cleaner Prod.*, 2024, **444**, 141287, DOI: [10.1016/j.jclepro.2024.141287](https://doi.org/10.1016/j.jclepro.2024.141287).
- 10 ISO-21338:2010, *Water quality – Kinetic determination of the inhibitory effects of sediment, other solids and coloured samples on the light emission of Vibrio fischeri 2010*, International Organization for Standardization, Geneva, Switzerland.
- 11 O. Bondarenko, K. Juganson, A. Ivask, K. Kasemets, M. Mortimer and A. Kahru, Toxicity of Ag, CuO and ZnO nanoparticles to selected environmentally relevant test organisms and mammalian cells in vitro: a critical review, *Arch. Toxicol.*, 2013, **87**, 1181–1200, DOI: [10.1007/s00204-013-1079-4](https://doi.org/10.1007/s00204-013-1079-4).
- 12 REACH: European Council, *Regulation (EC) No 1907/2006 of the EU Parliament and Council concerning the Registration, Evaluation, Authorisation and Restriction of Chemicals (REACH)*, 2006.
- 13 OECD-201, Test No. 201: Freshwater Alga and Cyanobacteria, Growth Inhibition Test 2011: OECD, DOI: [10.1787/9789264069923-en](https://doi.org/10.1787/9789264069923-en).
- 14 C. Caldeira, R. Farcas, C. Moretti, L. Mancini, H. Rauscher and K. Rasmussen, *et al.*, *Safe-and-Sustainable-by-Design chemicals and materials*, Publications Office of the European Union, Luxembourg, 2022.
- 15 OECD-202, Test No. 202: Daphnia sp. Acute Immobilisation Test 2004: OECD, DOI: [10.1787/9789264069947-en](https://doi.org/10.1787/9789264069947-en).
- 16 V. Aruoja, S. Pokhrel, M. Sihtmäe, M. Mortimer, L. Mädler and A. Kahru, Toxicity of 12 metal-based nanoparticles to algae, bacteria and protozoa, *Environ. Sci.: Nano*, 2015, **2**, 630–644, DOI: [10.1039/C5EN00057B](https://doi.org/10.1039/C5EN00057B).
- 17 OECD-235, Test No. 235: Chironomus sp., Acute Immobilisation Test 2011: OECD, DOI: [10.1787/9789264122383-en](https://doi.org/10.1787/9789264122383-en).
- 18 S. Suppi, K. Kasemets, A. Ivask, K. Künnis-Beres, M. Sihtmäe and I. Kurvet, *et al.* A novel method for comparison of biocidal properties of nanomaterials to bacteria, yeasts and algae, *J. Hazard. Mater.*, 2015, **286**, 75–84, DOI: [10.1016/j.jhazmat.2014.12.027](https://doi.org/10.1016/j.jhazmat.2014.12.027).
- 19 E. Vindimian, REGTOX EV7.1.2.xls MS-Excel Macro Software (accessed 14.06.2023), 2001, <http://www.normalesup.org/~vindimian/download.html>.
- 20 C. Blaise, F. Gagné, J. F. Féraud and P. Eullaffroy, Ecotoxicity of selected nano-materials to aquatic organisms, *Environ. Toxicol.*, 2008, **23**, 591–598, DOI: [10.1002/tox.20402](https://doi.org/10.1002/tox.20402).
- 21 O. M. Bondarenko, M. Heinlaan, M. Sihtmäe, A. Ivask, I. Kurvet and E. Joonas, *et al.* Multilaboratory evaluation of 15 bioassays for (eco)toxicity screening and hazard ranking of engineered nanomaterials: FP7 project NANOVALID, *Nanotoxicology*, 2016, **10**, 1229–1242, DOI: [10.1080/17435390.2016.1196251](https://doi.org/10.1080/17435390.2016.1196251).
- 22 F. Zhang, Z. Wang, W. J. G. M. Peijnenburg and M. G. Vijver, Review and Prospects on the Ecotoxicity of Mixtures of Nanoparticles and Hybrid Nanomaterials, *Environ. Sci. Technol.*, 2022, **56**, 15238–15250, DOI: [10.1021/acs.est.2c03333](https://doi.org/10.1021/acs.est.2c03333).
- 23 K. an Huynh, J. M. McCaffery and K. L. Chen, Heteroaggregation Reduces Antimicrobial Activity of Silver Nanoparticles: Evidence for Nanoparticle–Cell Proximity Effects, *Environ. Sci. Technol. Lett.*, 2014, **1**, 361–366, DOI: [10.1021/ez5002177](https://doi.org/10.1021/ez5002177).
- 24 F. Chen, L. Wu, X. Xiao, L. Rong, M. Li and X. Zou, Mixture toxicity of ZnO nanoparticle and chemicals with different mode of action upon *Vibrio fischeri*, *Environ. Sci. Eur.*, 2020, **32**, 41, DOI: [10.1186/s12302-020-00320-x](https://doi.org/10.1186/s12302-020-00320-x).



- 25 R. Bacchetta, N. Santo, M. Marelli, G. Nosengo and P. Tremolada, Chronic toxicity effects of ZnSO₄ and ZnO nanoparticles in *Daphnia magna*, *Environ. Res.*, 2017, **152**, 128–140, DOI: [10.1016/j.envres.2016.10.006](https://doi.org/10.1016/j.envres.2016.10.006).
- 26 J. R. Santos-Rasera, R. T. R. Monteiro and H. W. P. de Carvalho, Investigation of acute toxicity, accumulation, and depuration of ZnO nanoparticles in *Daphnia magna*, *Sci. Total Environ.*, 2022, **821**, 153307, DOI: [10.1016/j.scitotenv.2022.153307](https://doi.org/10.1016/j.scitotenv.2022.153307).
- 27 D. Ebert, *Ecology, epidemiology, and evolution of parasitism in Daphnia*, National Library of Medicine (US), National Center for Biotechnology Information, Bethesda, MD, 2005.
- 28 W. Wang, Y. Yang, L. Yang, T. Luan and L. Lin, Effects of undissociated SiO₂ and TiO₂ nano-particles on molting of *Daphnia pulex*: Comparing with dissociated ZnO nano particles, *Ecotoxicol. Environ. Saf.*, 2021, **222**, 112491, DOI: [10.1016/j.ecoenv.2021.112491](https://doi.org/10.1016/j.ecoenv.2021.112491).
- 29 E. Joonas, V. Aruoja, K. Olli, G. Syvertsen-Wiig, H. Vija and A. Kahru, Potency of (doped) rare earth oxide particles and their constituent metals to inhibit algal growth and induce direct toxic effects, *Sci. Total Environ.*, 2017, **593–594**, 478–486, DOI: [10.1016/j.scitotenv.2017.03.184](https://doi.org/10.1016/j.scitotenv.2017.03.184).
- 30 C. Gao, K. A. C. de Schampheleere and E. Smolders, Zinc toxicity to the alga *Pseudokirchneriella subcapitata* decreases under phosphate limiting growth conditions, *Aquat. Toxicol.*, 2016, **173**, 74–82, DOI: [10.1016/j.aquatox.2016.01.010](https://doi.org/10.1016/j.aquatox.2016.01.010).
- 31 X. Li, J. Li, Z. Wang, R. Bol and H. Zou, Heteroaggregation of carbon nanomaterials with mineral-based nanomaterials: A review, *J. Environ. Chem. Eng.*, 2024, **12**, 113594, DOI: [10.1016/j.jece.2024.113594](https://doi.org/10.1016/j.jece.2024.113594).
- 32 USEPA, *United States Environmental Protection Agency: National Recommended Water Quality Criteria – Aquatic Life Criteria Table*, 2025.
- 33 Canadian BC Ministry of Environment, *British Columbia Water Quality: Ambient Water Quality Guidelines for Zinc*, Overview Report, 1999.
- 34 C. Shen, S. A. James, M. D. de Jonge, T. W. Turney, P. F. A. Wright and B. N. Feltis, Relating cytotoxicity, zinc ions, and reactive oxygen in ZnO nanoparticle-exposed human immune cells, *Toxicol. Sci.*, 2013, **136**, 120–130, DOI: [10.1093/toxsci/kft187](https://doi.org/10.1093/toxsci/kft187).

